

Institut für Plasmaphysik
KERNFORSCHUNGSANLAGE JÜLICH
des Landes Nordrhein-Westfalen

Production of a Highly Ionized Plasma with Low
Impurity Level, with and without Magnetic Bias Fields
for Magnetic Compression Experiments

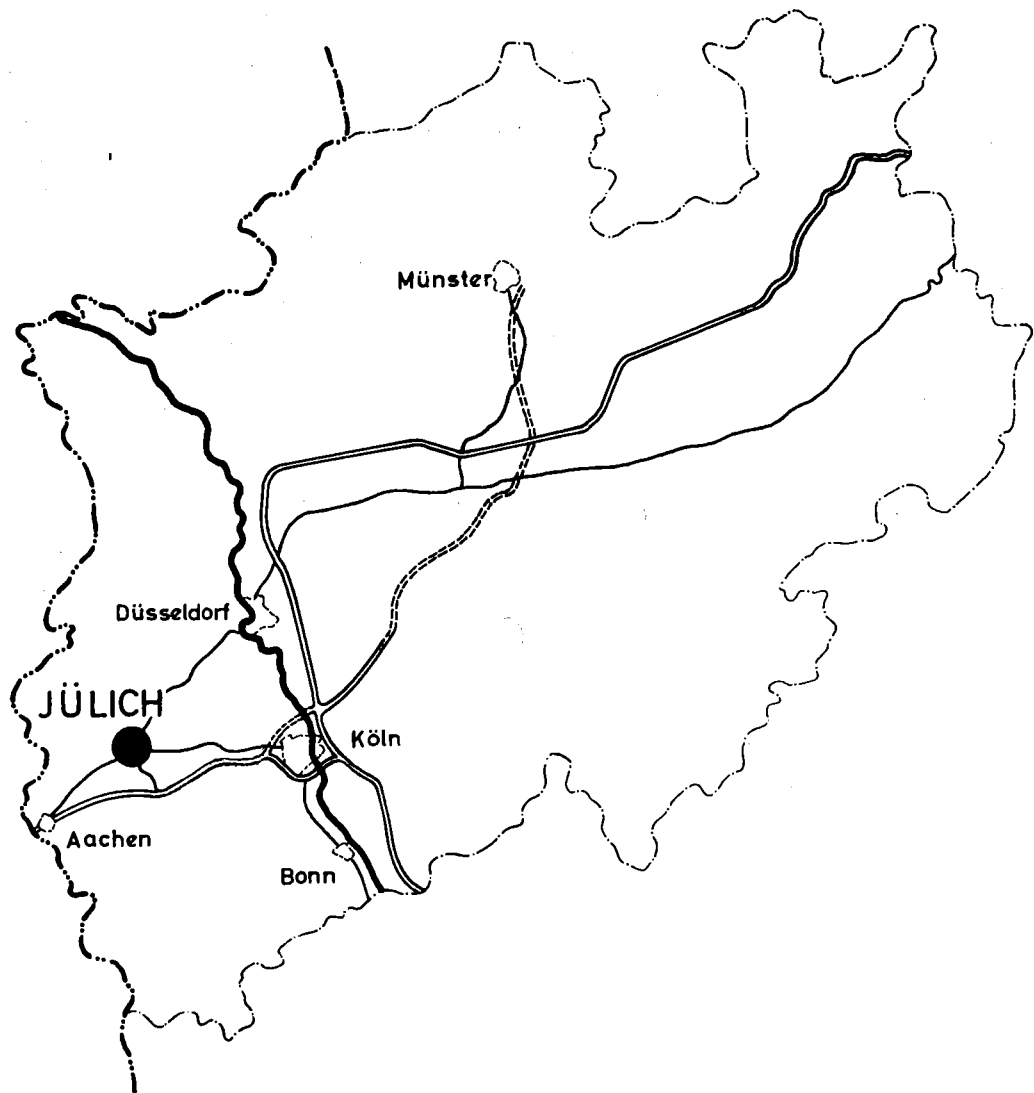
by

H. Beerwald, P. Bogen,
T. El-Khalafawy, H. Fay,
E. Hintz and H. Kever

Jül - 19 - PP

August 1961

Als Manuskript gedruckt



Berichte der Kernforschungsanlage Jülich – Nr. 19

Institut für Plasmaphysik Jül – 19 – PP

Dok.: PLASMA-MAGNETIC COMPRESSION * DK 533.21-128 : 538.652

Zu beziehen durch: ZENTRALBIBLIOTHEK der Kernforschungsanlage Jülich
Jülich, Bundesrepublik Deutschland

Production of a Highly Ionized Plasma with Low Impurity Level,
with and without Magnetic Bias Fields for Magnetic Compression

Experiments,

by

H. Beerwald, P. Bogen, T. El-Khalafawy, H. Fay, E. Hintz

and H. Kever*

Institut für Plasmaphysik der Kernforschungsanlage Jülich des
Landes Nordrhein-Westfalen e.V. Jülich/Germany

1. Introduction

For the compression of a cylindrical plasma by fast rising axial magnetic fields, the initial state of this plasma is of critical importance (1). Therefore experiments with a preheating discharge for the production of an initial plasma with known and reproducible properties were started at this laboratory simultaneously with the first experiments on the compression of a weakly preionized deuterium gas.

An electrodeless ring discharge was chosen. The absence of electrodes makes a high degree of purity of the plasma possible.

Kolb's experience with a preheating discharge for magnetic com-

*Paper presented at the Conference on Plasma Physics and Controlled Nuclear Fusion Research, Salzburg 1961.

pression experiments (2) confirmed this conception and gave further impulse to this work.

Early experiments were made with a RF-transmitter as current generator, in pulsed as well as in stationary operation. Due to the low inductance of the compression coil considerable difficulties are met in coupling the RF power to the discharge. The maximum available power is limited to some hundred kilowatts.

By discharging a low inductance condenser on the compression coil a damped RF pulse with a power of 100 M Watt is easily obtained. To avoid prefiring of the main condenser bank, the voltage of the coil must be limited. With the spark gaps used at this laboratory the maximum permissible voltage at the coil was about 5 kV. This voltage, however, is sufficient to start an electrodeless ring discharge in hydrogen.

Investigations on this electrodeless ring discharge were made with and without a steady magnetic bias field in a wide pressure range. Preliminary results, concerning the breakdown of the gas, the formation of a highly ionized plasma, and the subsequent decay of the plasma due to end losses and recombination are reported in this paper.

2. Diagnostic Methods.

For the formation and the decay of the plasma electron temperature and electron density are of main interest. The appropriate diagnostic method for the measurement of these quantities depends on the range of temperatures and densities expected.

Between 10^{10} - 10^{13} electrons/cm³ electron density and density changes were measured with an 8,5 mm microwave interferometer(3). Above 10^{15} electrons/cm³ the electron density was determined by Stark broadening of H_β. The profile of H_β is well known from theoretical (4) and experimental work (5). N_e can be determined experimentally from the half width of this line. This half width can be obtained by measuring the intensity as a function of time for various distances from the line centre, at consecutive discharges.

Above 2 eV the electron temperature was determined by the relative intensities of C II (4267 Å) and C III (2297 Å) spectral lines, as described elsewhere (6).

Below 2 eV an estimate of the electron temperature can be obtained at the intensity maximum of H_β, if the plasma is not be-

ing compressed.

Magnetic probe measurements give additional information on the heating mechanism and on the homogeneity of the plasma. From measured magnetic field distributions one gets the skindepth and the magnetic pressure gradient, the electron temperature and the particle density can be derived therefrom.

3. Experimental Arrangement.

A single turn, cylindrical compression coil of 40 mm inner diameter and 150 mm length is used both for the generation of the alternating magnetic field and of the steady magnetic field. The discharge tube of 2 mm wall thickness and 600 mm length is closely fitted to the coil.

A diagram of the electric circuit is shown in fig.1. The current generator for the steady magnetic field is an artificial delay line, terminated by its impedance, which produces a nearly rectangular current pulse. The duration of the pulse is about 100 μ sec, the risetime 4 μ sec and the maximum current 35 000 A, the maximum B-field correspondingly 3 000 Gauss. By discharging C_1 an oscillating magnetic field with a maximum amplitude of

5 000 Gauss, an oscillation frequency of 900 kc sec^{-1} and a damping constant of $2.6 \mu\text{sec}$ can be produced.

4. Results.

In an electrodeless ring discharge the electrons are moving in crossed electric and magnetic fields, in contrast to many other types of discharges. This strongly influences ionization growth, in particular at low pressures. Assuming $\nu_e < \nu_c$ (ν_e = electron-atom collision frequency, ν_c = electron cyclotron frequency) and $\omega \ll \nu_e$ (ω = resonance frequency of the discharge circuit), the energy transfer to the electrons can be calculated for times of the order $\frac{1}{\nu_c}$ (7).

Assuming a sinusoidal magnetic field, two time intervals can be distinguished

$$1) \quad \frac{1}{\nu_c} \cdot \frac{1}{B} \cdot \frac{dB}{dt} > 1 \qquad 2) \quad \frac{1}{\nu_c} \cdot \frac{1}{B} \cdot \frac{dB}{dt} < 1$$

Case (1): The electron obtains a maximum velocity of about

$$V_m \approx 1.6 \cdot \frac{r}{2} \omega_c^{\frac{1}{2}} \qquad , \text{ at a time } t_m \approx 2 \cdot \omega_c^{-\frac{1}{2}} \qquad , \text{ where}$$

$\omega_c = 2\pi \nu_c$. The corresponding energy of the electron is

$$E \approx \frac{1}{10} U \text{ (eV)}, \text{ where } U \text{ is the voltage at the coil. From this}$$

relation one gets an estimate for maximum ionization growth due

to this mechanism

$$n_e \approx n_{e0} \frac{U}{30 U_i},$$

where n_{e0} is the initial electron density and U_i the ionization energy.

Case (2): Two cases can be distinguished:

a) $\omega_c (T) > \omega_p$; ω_p = plasma frequency

T = time since the start of the discharge.

The maximum velocity is $2 \cdot \frac{E}{B}$, which means that the electron energy can exceed the ionization energy only for times of the order 10^{-8} sec in the experiment described above.

b) $\omega_c (T) < \omega_p$

The electron velocity tends to $\frac{\dot{\omega}_c r t}{2} \sim E \cdot t$. In contrast to the other cases, the velocity increases linearly with time.

Ionization can therefore proceed as long as the E-field is high enough.

The main conclusion from these results is that a good preionization of the gas, resulting in a high initial electron density and plasma frequency, is essential for the fast growth of ionization.

For the breakdown of the gas with a steady magnetic bias field the sign and the magnitude of the ratio $K = \frac{B_{\text{steady}}}{B_{\text{pulsed}}}$ are of importance.

In order to obtain favourable conditions for breakdown in the first halfcycle, it is necessary

- 1) to choose the negative sign for K,
- 2) to choose K smaller than 1, because $\frac{E}{B}$ stays small for $K \geq 1$.

A rapid ionization will not occur in either of the cases (2a), (2b).

This can be confirmed by measurements. Fig.2 shows oscilloscope traces of the microwave signal for two typical cases at $50 \mu D_2$.

case (a): $K = - 1/2$ $\omega_p = 10^{10} \text{sec}^{-1}$.

About $0.1 \mu\text{sec}$ after the maximum of E_{θ} the cyclotron frequency of the electrons becomes smaller than the plasma frequency and a short time later the magnetic field goes through zero. In this time interval there should be a rapid increase in electron density. This is in good agreement with the experimental results. Within $2 \cdot 10^{-7} \text{sec}$ the electron density increases by a factor of 100.

case (b): $K = 0$. $\omega_p \ll 10^{10} \text{ sec}^{-1}$.

This picture shows the importance of a high initial electron density for the breakdown of the gas. The first two half cycles of the discharge are used to build up an electron density of about $5 \cdot 10^{10} - 10^{11} \text{ cm}^{-3}$, which in the other case exists already at the start of the discharge. At the following fourth voltage maximum the gas breaks down.

2) Development of the plasma after breakdown.

Most of the measurements have been made at an initial pressure of $230/\mu \text{ H}_2$ without a magnetic bias field, this being the most interesting case for present compression experiments at this laboratory. It could be shown, however, that with other interesting sets of initial parameters the maximum electron temperature and ionization degree in the plasma are not essentially different.

Fig.3 shows photomultiplier traces of C II and C III lines and the temporal development of the electron temperature, derived from their relative intensities at $230/\mu \text{ H}_2$.

The plotted curve gives a minimum value of T_e . The true electron

temperature is probably higher due to incomplete equilibrium and nonuniform distribution of the electron temperature.

Magnetic field measurements can give information on the homogeneity of the plasma. Fig.4 shows the internal and external field at $230/\mu$ and at $120/\mu$ D_2 . The magnetic field signals at these two pressures are very similar and show clearly that during the third current half cycle internal and external fields are of opposite sign, with high magnetic field gradients in between.

These are produced by strong currents giving a sudden increase of electron temperature.

Fig.5 shows a set of magnetic field distributions during the interdiffusion and heating phase in the third halfcycle and the following more stationary phase at $120/\mu$ D_2 . From fig.5e one obtains the conductivity of the plasma $2.2/\mu\text{sec}$ after the start of the discharge. The electron temperature derived from the conductivity is about 3 eV, at least in the boundary zone. Because the electron-ion collision frequency at these densities is of the order 10^8sec^{-1} , the ion temperature should be approximately equal to the electron temperature. Assuming that the plasma temperature near the axis is much lower than 3 eV, a pressure front should travel towards the axis with a velocity

of about 2 cm/ μ sec. After 1/ μ sec the magnetic field distribution should then clearly show a displacement of the plasma boundary. This displacement is not observed.

Smear camera pictures likewise show that in this time interval velocity changes of the plasma boundary are negligible. Therefore inertial effects can be neglected and the external magnetic pressure is balanced by the kinetic pressure. Assuming the particle density to be 10^{16} particles per cc, one derives a plasma temperature of about 18 000 $^{\circ}$ K fig. 5g.

At 230/ μ H₂ the electron density was measured by Stark broadening of H _{β} . Fig.6 shows a photomultiplier trace at the centre of H _{β} and at $\Delta\lambda = 5\text{\AA}$. The half width of H _{β} and the calculated electron density as a function of time is shown in fig.7.

3/ μ sec after the start of the discharge a half width of 12 \AA was measured, which corresponds to an electron density of $1.4 \cdot 10^{16} \text{ cm}^{-3}$. From streak camera pictures the maximum volume compression was estimated to be smaller than 2:1. Therefore the degree of ionization at that time is higher than 50%, probably near 100%.

The percentage of carbon in the "pure" hydrogen plasma was ob-

tained by comparing the photomultiplier traces of C II and C III lines in initially pure hydrogen and in $H_2 + \frac{1}{760} CH_4$. The carbon line intensities in the latter case are a factor of three higher. The concentration of carbon in the plasma was then estimated to be 0.02%. For oxygen a value of the same order of magnitude was obtained. The impurity degree was not constant but always below a value of 0.05%.

Both streak camera and magnetic field measurements indicate that the plasma is fairly uniformly distributed after about 5 μ sec. With the assumption that at this time the degree of ionization is above 50% one would expect a maximum of H_β after some time. Fig. 8 shows the intensity of H_β as a function of time at an initial pressure of 230 μ . The maximum appears after about 11 μ sec, indicating a temperature of about 13 000°K at this time.

Further investigations on the electrodeless ring discharge were made at 60 μ and 500 μ without superimposed steady magnetic field and at 230 μ with steady magnetic fields of various amplitudes and a field direction opposite to the pulsed field during the first half-cycle (8).

The measured maximum electron temperatures are compiled in the

following table:

P_0	=	50	230	500	230	230 μ
B_0	=	0	0	0	1 200	2 400 Gauss
T_e	=	27 000	22 000	16 000	32 000	27 000 $^{\circ}\text{K}$

H_{β} intensity and magnetic field measurements show in all cases that the electron temperature is higher than $13\,000^{\circ}\text{K}$ at the time when plasma and magnetic field are nearly homogeneously distributed. However with a superimposed steady magnetic field it takes much more time to reach this phase.

The time needed to obtain a reasonably uniform radial distribution of plasma and magnetic field, must be compared with the characteristic time for end losses $\tau \sim \frac{l}{v}$, where v is the sound velocity in the plasma and l the length of the coil. If these two times are comparable then the particle density differs appreciably from the initial particle density and should be nonuniform along the axis. This is demonstrated by fig.7 which shows the changes in electron density due to end losses.

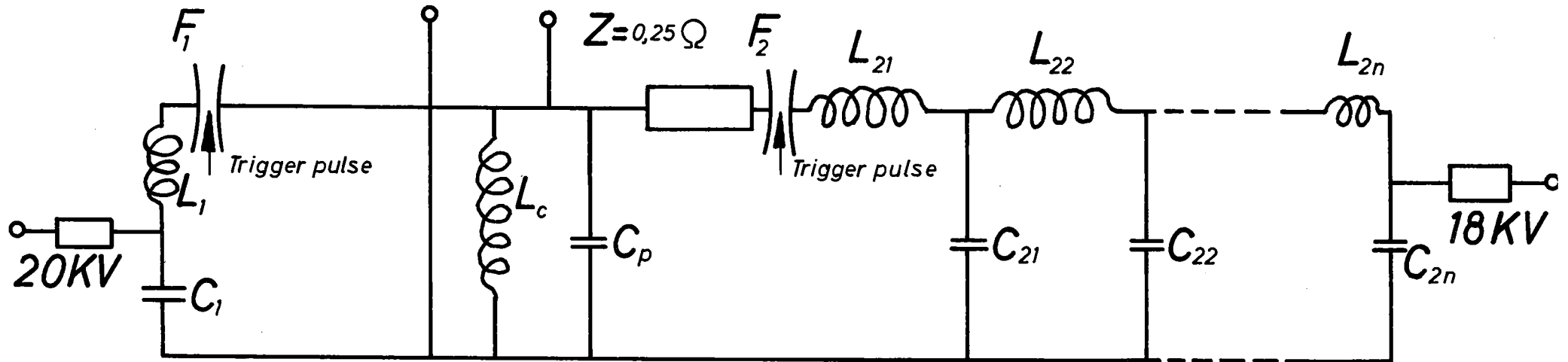
Experiments also show that end losses are influenced by the presence of an internal field. To fix the initial conditions for a magnetic compression experiment, the particle density for each

set of initial conditions therefore must be measured separately at the appropriate time.

References:

- 1) Jordan, H.L., Conference on Plasma Physics and Controlled Nuclear Fusion Research, Salzburg, 1961.
- 2) Kolb, A.C., Proceedings of the Second United Nations International Conference on the peaceful Uses of Atomic Energy, 31, Geneva 1958, 328.
 Kolb, A.C., et al., Proceedings of the Fourth International Conference on Ionization Phenomena in Gases, Uppsala 1959, 1037.
- 3) Beerwald, H., Fifth International Conference on Ionization Phenomena in Gases, München, 1961.
- 4) Griem, H.R., et al., Phys. Rev. 116, (1959) 4.
- 5) Bogen, P. Z. Physik, 149, (1957) 62.
- 6) El-Khalafawi, T., Bogen, P., to be published.
 El-Khalafawi, T., Thesis, TH. Aachen, 1961.
- 7) Bodin, H.A., Green, T.S., et al., Proceedings of the Fourth International Conference on Ionization Phenomena in Gases, Uppsala 1959, 1065.
- 8) Bogen, P., Hintz, E., Proceedings of the Fifth International Conference on Ionization Phenomena in Gases, Munich, 1961.

To Main Condenser Bank



C_p = Capacitance of Collector-plate

C_1 = Capacitance of Preheat-condenser

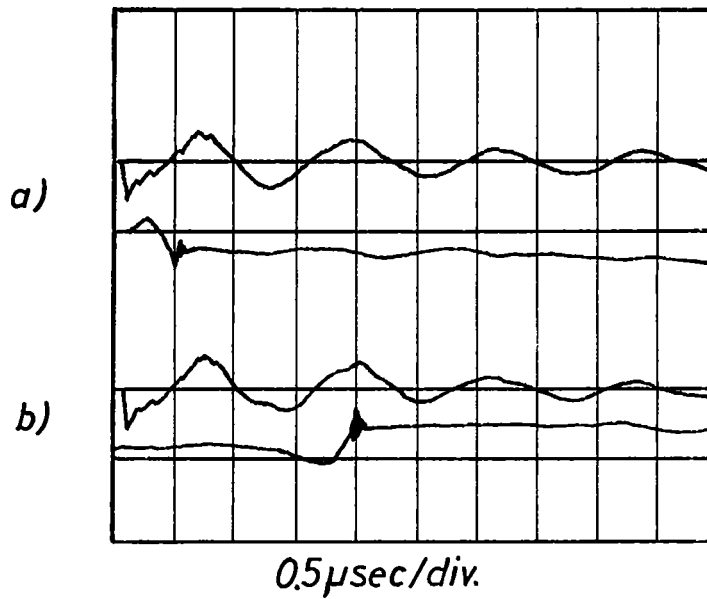
$C_{21} \dots C_{2n}$ } Inductances and Capacitances

$L_{21} \dots L_{2n}$ } of Artificial Delay Line

L_c = Inductance of Discharge Coil

Electrical Circuit Diagram

Fig.1



a) $K = -\frac{1}{2}$; $\omega_p \approx 10^{10} \text{ sec}^{-1}$

b) $K = 0$; $\omega_p \ll 10^{10} \text{ sec}^{-1}$

Upper trace: voltage at the coil

Lower trace: microwave interferometer signal

Ionization growth at $50 \mu D_2$

Fig. 2

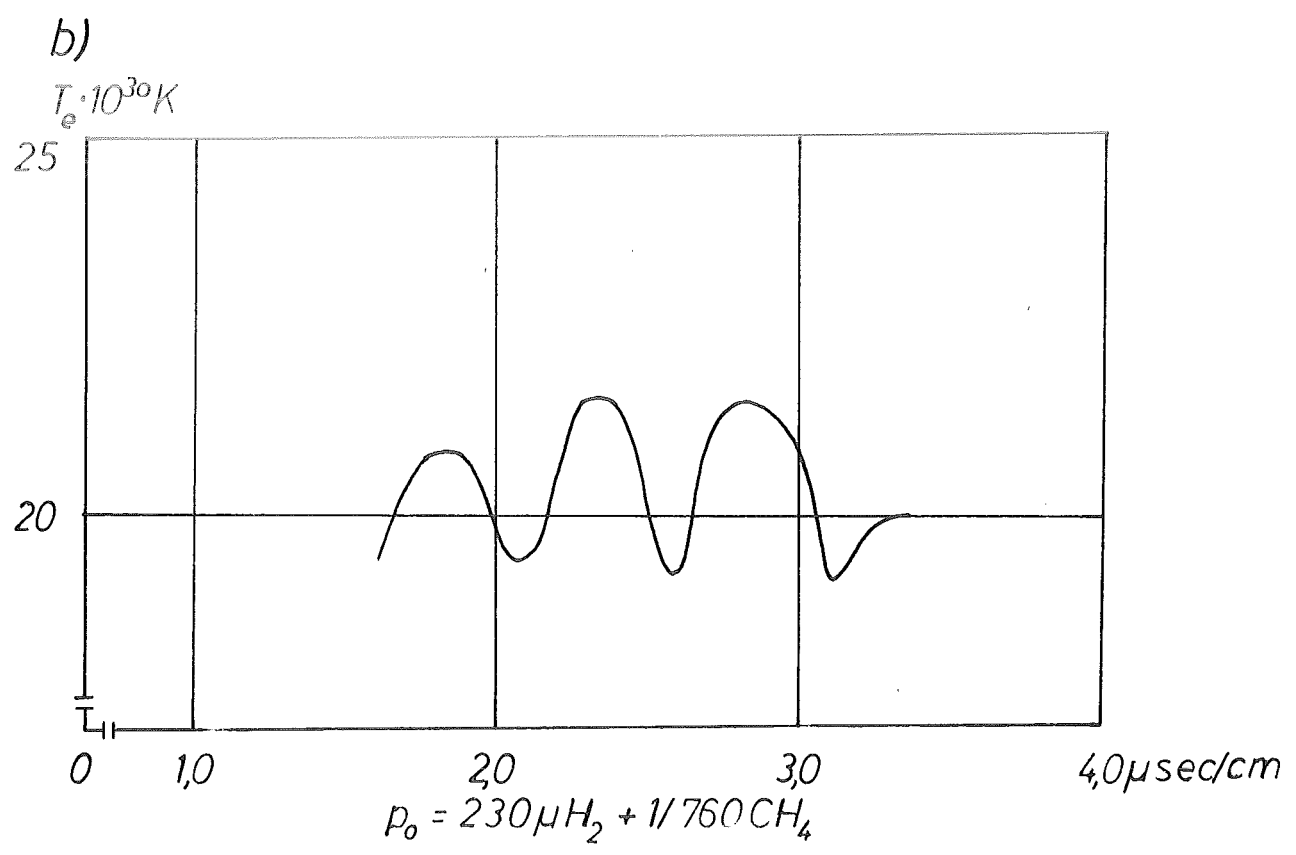
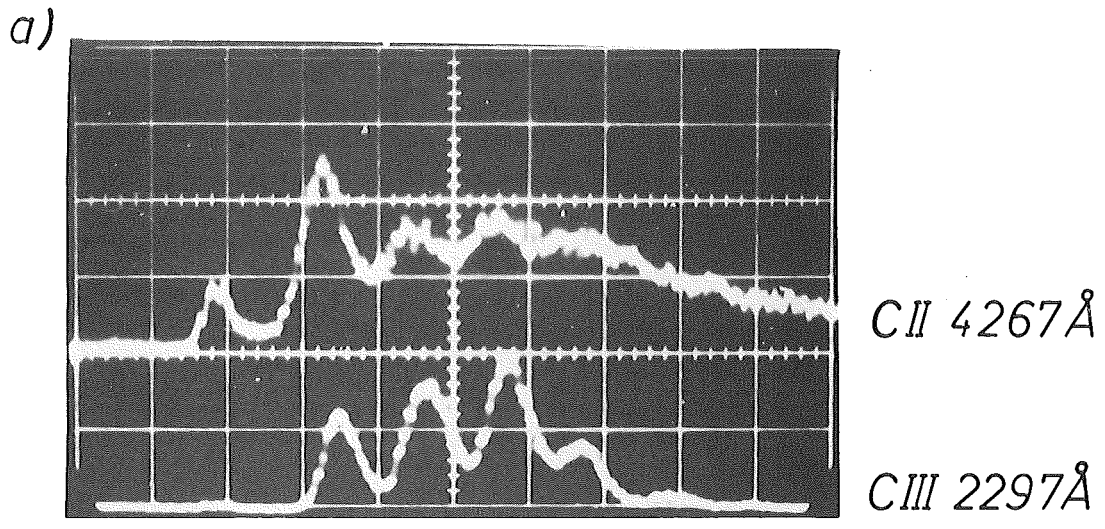


Fig. 3a CII and CIII spectral line intensity as function of time.
 3b Electron temperature as a function of time.

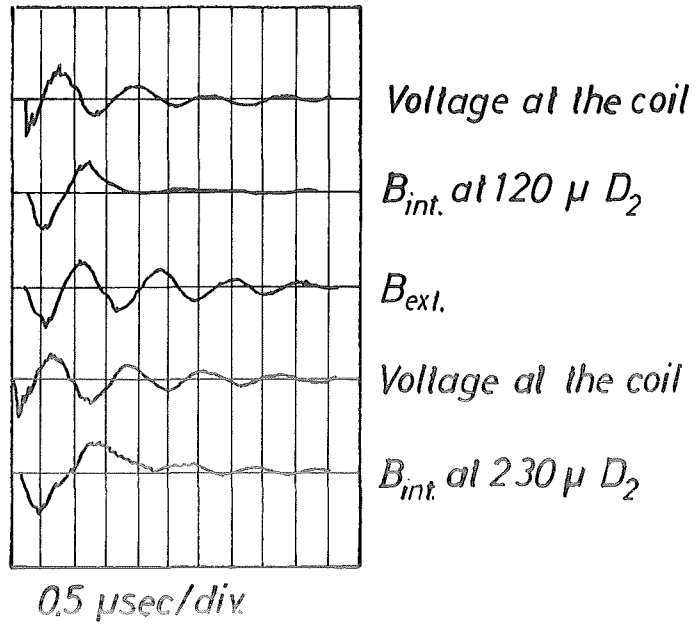
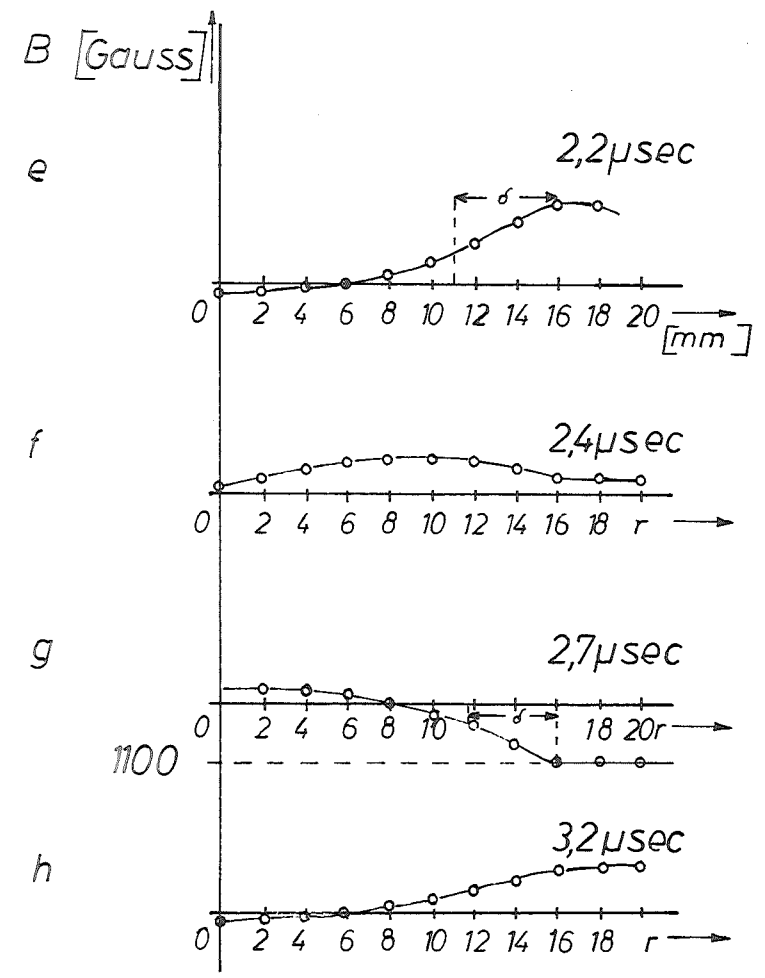
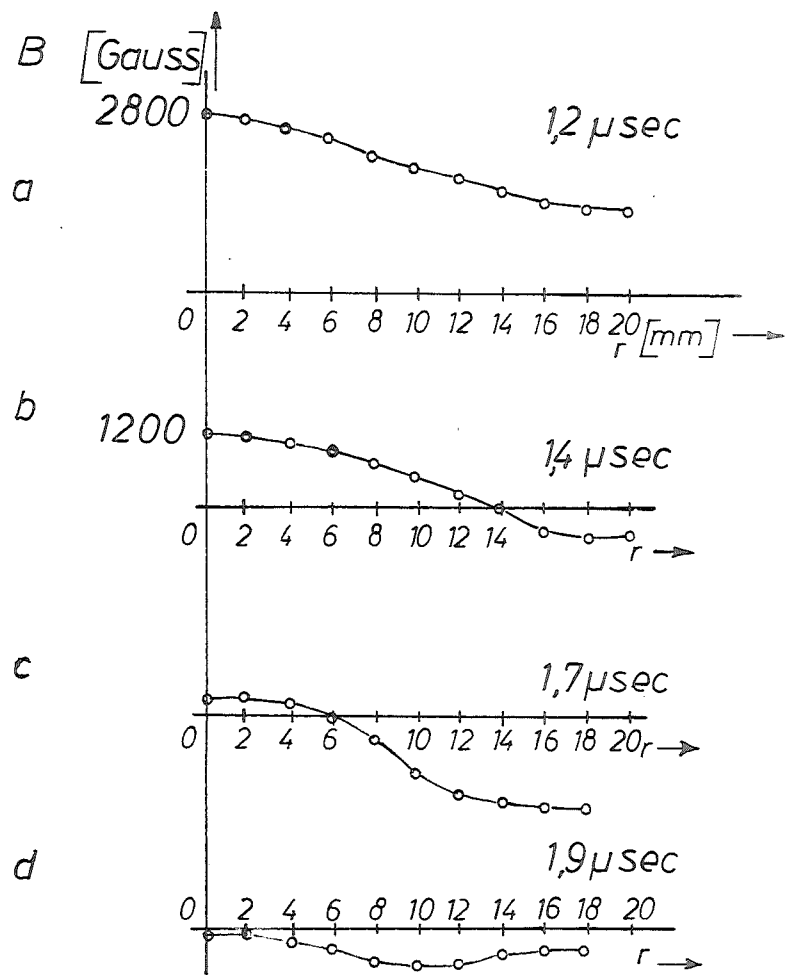


Fig.4 $B_{int.}(t)$ and $B_{ext.}(t)$ at $230 \mu D_2$ and at $120 \mu D_2$.

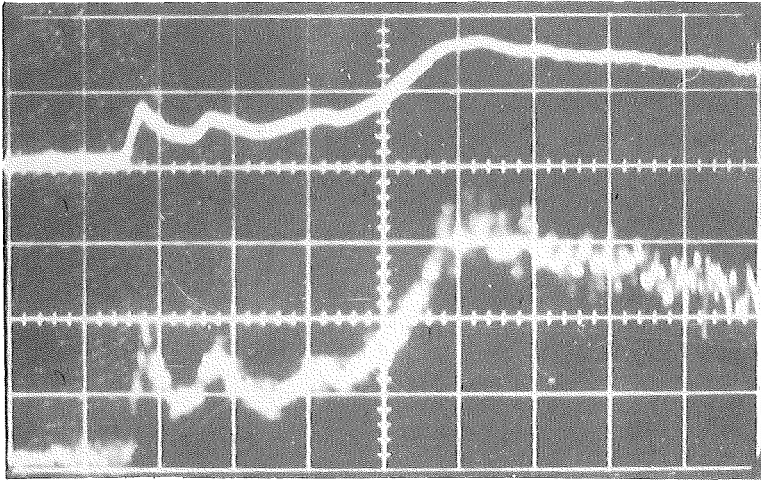


$$P_0 = 120 \mu D_2$$

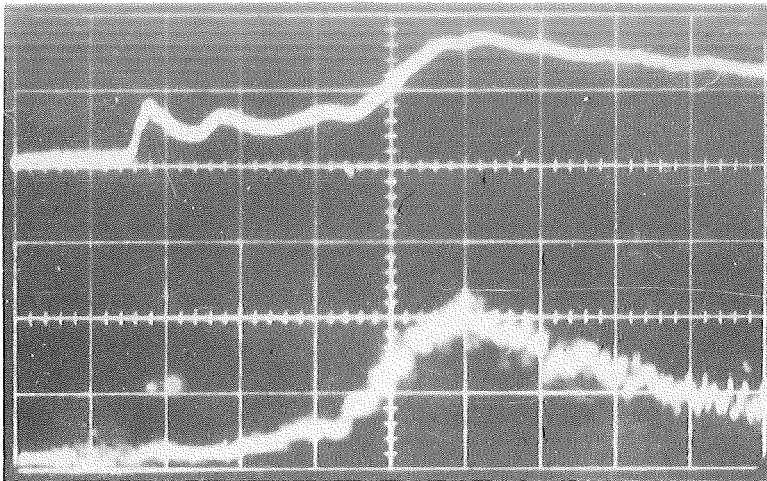
Radial Magnetic Field Distribution as a Function of Time

Fig. 5

a)



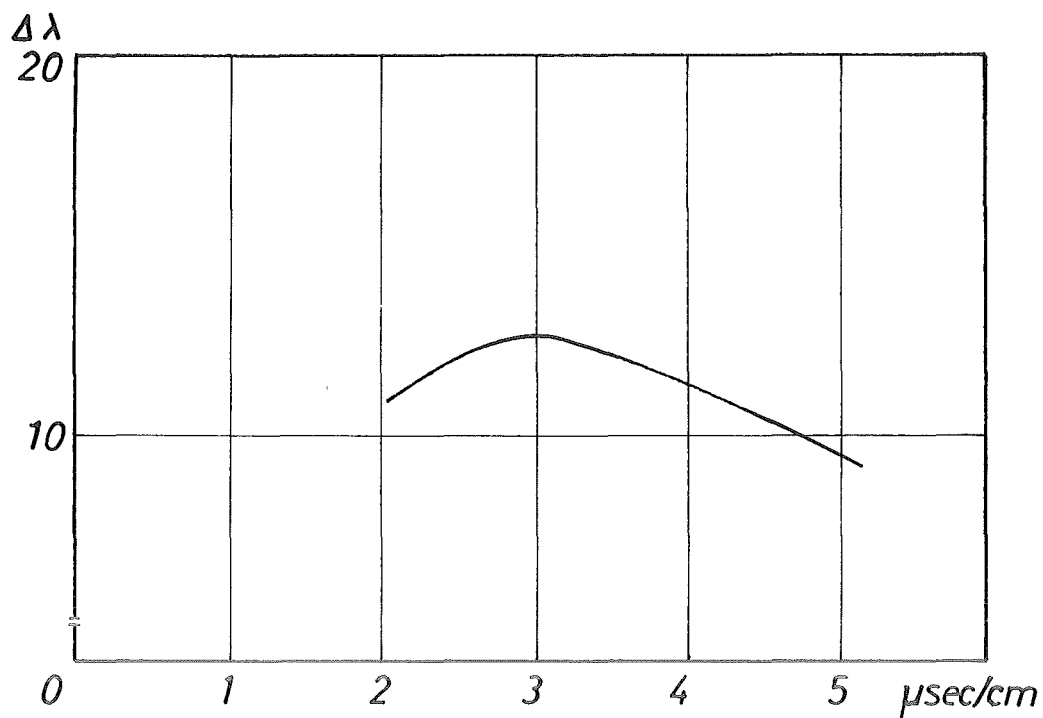
b)



Time scale 0,5 μ sec/div.

Fig.6 H_{β} line intensity in the line centre (a) and at $\Delta\lambda = 5\text{\AA}$ (b).

a)



b)

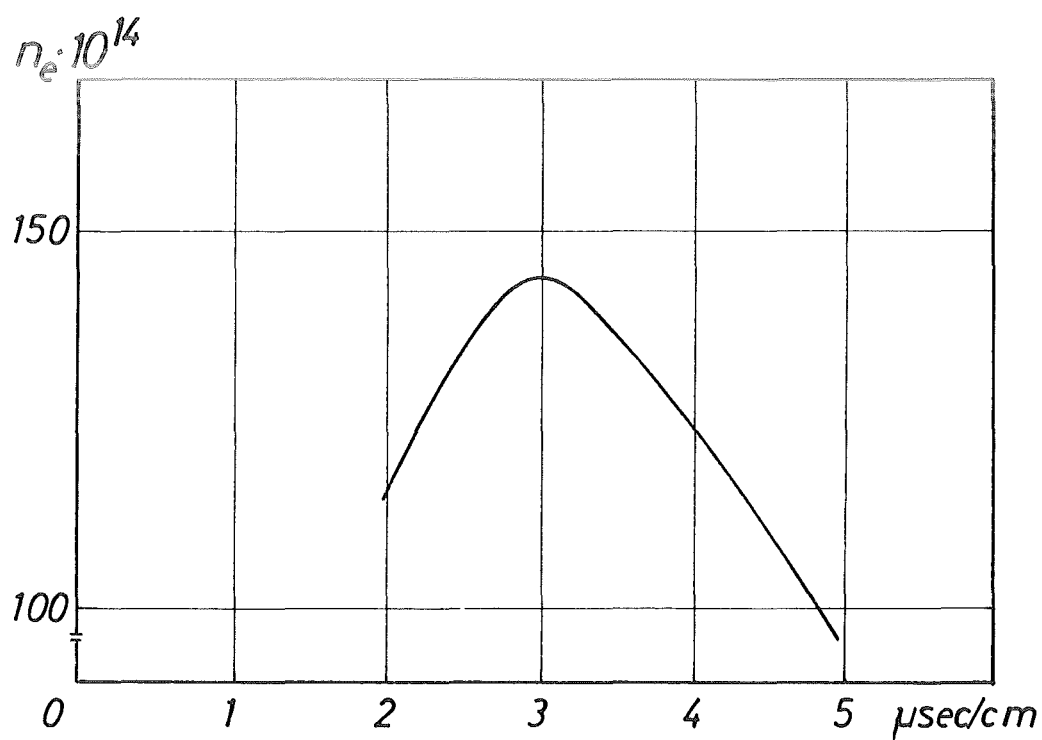
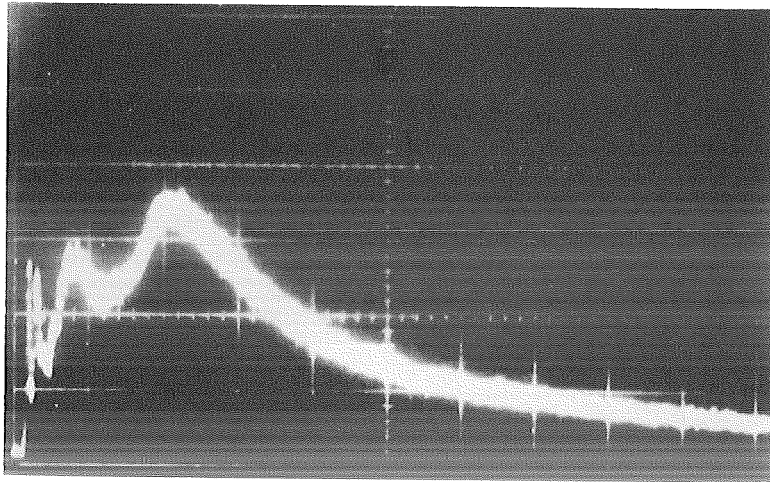


Fig. 7a Half-width of H_β as a function of time.

7b Electron density as a function of time.



Time scale $5\mu\text{sec/div}$.

*Fig.8 D_β intensity as a function
of time.*